Lawrence Berkeley Laboratory
UNIVERSITY OF CALIFORNIA

EARTH SCIENCES DIVISION

Presented at the 13th Workshop on Geothermal Reservoir Engineering, Stanford, CA, January 19–21, 1988

Mathematical Modeling of Near-Critical Convection

B.L. Cox, K. Pruess, and R. McKibbin

January 1988

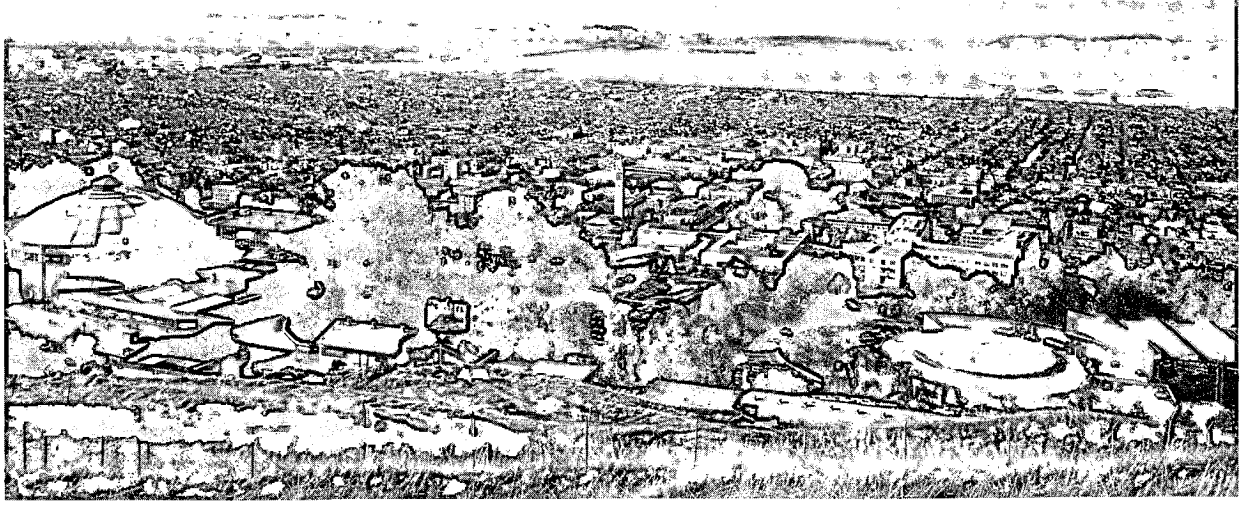

Prepared for the U.S. Department of Energy under Contract DE-AC03-76SF00098

DISCLAIMER

MATHEMATICAL MODELING OF NEAR-CRITICAL CONVECTION

B. L. Cox, K. Pruess, and R. McKibbin*

Earth Sciences Division, Lawrence Berkeley Laboratory
University of California, Berkeley, California 94720

*On leave from Geothermal Institute, University
of Auckland, Private Bag, Auckland, New Zealand

ABSTRACT

Fluid and heat flow at temperatures approaching or exceeding that at the critical point (374°C for pure water, higher for saline fluids) may be encountered in deep zones of geothermal systems and above cooling intrusives. Laboratory experiments have demonstrated strong enhancements in heat transfer at near-critical conditions (Dunn and Hardee, 1981).

We have developed special numerical techniques for modeling porous flow at near-critical conditions, which can handle the extreme non-linearities in water properties near the critical point. Our numerical experiments show strong enhancements of convective heat transfer at near-critical conditions; however, the heat transfer rates obtained in the numerical simulations are considerably smaller than those seen in the laboratory experiments by Dunn and Hardee. We discuss possible reasons for this discrepancy and develop suggestions for additional laboratory experiments.

INTRODUCTION

Fluid conditions approaching or exceeding the critical point (374°C, 221 bars for pure water; higher temperatures and pressures for saline brines) may be reached in the deep ends of geothermal systems such as Mofete (Facca, 1985) and Larderello (Cappetti et al., 1985), as well as above crustal magma bodies. Yet, little is known about how heat and fluid flows are affected by critical conditions. In order to better evaluate geothermal reservoirs with critical conditions at depth, and to estimate heat and fluid flows in critical zones above magma bodies, we need to better understand the behavior of geothermal fluids near the critical point.

Previous studies include one by Cathles (1977) who used a finite difference model to study cooling igneous intrusives and the formation of liquid- and vapor-dominated geothermal systems, as well as the formation of porphyry-type ore deposits. He concluded that fluids circulate around the critical point of water to become gaseous without boiling, and that these zones are potentially exploitable. Norton and Knight (1977) also performed finite difference simulations of cooling plutons; they found that the style of circulation was controlled by the critical fluids and that the total heat flow calculations can be significantly in error if these convecting zones are not considered.

Laboratory experiments of natural convection of critical fluids in a porous medium were performed by Dunn and Hardee (1981) for water, and by Hadley (1982) for carbon dioxide. Dunn and Hardee found that heat transfer rates increased by factors of up to 70 when compared to conductive heat flow near the critical point of water, and attributed this enhancement to the extreme behavior of fluid properties (especially density and heat capacity) in the critical region. Hadley (1982) found substantial heat transfer enhancement (Nusselt number of 12) for carbon dioxide, and concluded that thermal dispersion was very important because of high fluid velocities generated near the critical point.

Above critical temperatures and pressures, there are no longer distinct liquid and gas phases, but instead a continuous variation from liquid-like fluid to gas-like fluid. This supercritical fluid has an enhanced ability to transport heat by convection because of the extreme behavior of fluid properties such as density and heat capacity. Contours of density and of internal energy at near-critical temperatures and pressures are plotted in Figures 1a and 1b. These plots were made by using a table generated from the Haar equation of state for water (Haar et al., 1984). The rapid changes in values indicated by the bands of compression of contours show one of the many problems occurring when trying to model a system with such non-linear behavior.

NUMERICAL MODELING OF NEAR–CRITICAL FLOW

Simulations were performed with the geothermal reservoir simulator MULKOM (Pruess, 1983), utilizing the Haar equation of state for water (Haar et al., 1984). Non-linearities in the water properties near the critical point create problems for numerical models, necessitating the development of new techniques. One of the modifications made in MULKOM was the use of a table of densities and internal energies as functions of temperature and pressure in the critical region. For every time step, these values are called, and used as starting values for the energy and mass flow calculations. A bi-linear interpolation scheme is used to estimate values between table values.

A second problem resulted from large pressures near the critical point (of the order 10^7 Pa) which are accompanied by very small pressure differences (of the order 10 Pa) between neighboring volume elements in a finite difference grid. This problem was overcome by using a floating reference pressure (average pressure in the flow system at each time step) so that more significant figures could be retained.

A third problem was encountered when a thermal convection problem was initialized with uniform temperature everywhere except at the heat source. This method of initializa-

tion gave rise to many transient flow reversals and was very slow and costly in computer time. In the present work we are only interested in the steady state attained after all transient changes have disappeared. To speed up the approach to steady state, we initialized the simulations by generating a set of temperatures corresponding to pure conduction between the heat source and the outer constant temperature boundary. This conductive steady state initialization greatly improved the efficiency of the simulations.

There is still a need to incorporate further modifications into MULKOM for near-critical convection. Thermal dispersion, flow channeling, and near-critical phase transitions may all be important, depending on the type of problem studied.

CODE VALIDATION AND NUMERICAL EXPERIMENTS

Before the simulator can be used to model geologic systems, it needs to be validated against some experimental data. The only available experimental work on near-critical porous convection of water is the one performed at Sandia National Laboratories (Dunn and Hardee, 1981). A conceptual sketch of the experimental setup is shown in Figure 2. A 1 liter cylindrical vessel filled with a fine silica sand was heated with electrical tape heaters on the cylinder mantle, and along a thin platinum wire in the center of the vessel. The outside of the cylinder was kept at a somewhat lower temperature than the wire, and the top and bottom of the cylinder were insulated. The steady-state temperatures were measured with embedded thermocouples, and a measure of the total heat transfer divided by conductive heat transfer (Nusselt number, Nu) was estimated. The experimenters found an enhancement in heat transfer over a broad temperature range from 360 to 400°C, which near the critical point reached a peak of about 70 times that for pure conduction.

Dunn and Hardee (1981) presented calculations of Rayleigh numbers (Ra) for parameters representative of their experiment, using a hypothetical temperature difference of 2°C between the wire and the cylinder mantle. They found a narrow peak centered at 374°C with maximum Rayleigh number of Ra = 700. The experimental measurements, when plotted as rate of heat transfer per unit temperature drop between two measurement points in the vessel, showed a temperature dependence similar to that of the calculated Rayleigh numbers. This correspondence led Dunn and Hardee to suggest that the enhanced heat transfer near the critical point was in fact brought about by the enhanced convective heat transport. However, this correspondence (Ra-Nu) should be viewed in a qualitative rather than quantitative sense because the calculated Ra are much too small to explain the observed heat transfer enhancements by factors up to 70 (Prasad et al., 1985; Reda, 1986).

Furthermore, a Rayleigh number based on temperature differences between hot and cold boundaries is not a very meaningful measure of convective heat transfer in a flow system with cylindrical symmetry, because temperature behaves in a singular fashion near the symmetry axis. We believe that fairly large temperature differences (substantially larger than 2°C) must have been present in the experiments. The precise location of the temperature sensors is not given by Dunn and Hardee, but from the sketch in the paper, it appears that the temperature measurements were made at the mid-height of the vessel, and none were made next to the wire. When convection occurs, a thin boundary layer would form next to the wire, and the pattern of convection would be asymmetrical in the vertical, so that measuring temperature differences at mid-height and away from the wire would not give quantitatively accurate estimates of the Nusselt number. A second reason for believing that temperature differences in the experiment must have been substantially larger than 2°C is that measured heat transfer is strongly enhanced over a rather broad temperature interval (from 360 to 400°C), while the peak in the Rayleigh numbers (for a 2°C temperature difference) is very narrow and steep right at the critical temperature.

We conclude that the Sandia experiment does not provide a sufficiently detailed definition of thermodynamic conditions to permit a careful code validation. Using the flow geometry shown in Figure 2, we performed a series of numerical experiments (Tables 1 and 2) to study various issues relating to near-critical heat transfer, such as the effects of boundary conditions, aspect ratio of convecting cells, discretization, and size of temperature interval. Our initial simulations gave rather weak enhancements in overall heat transfer, and specific efforts were made to obtain a more enhanced heat transfer, using flow geometry and parameters similar to those of the experiment. The two-dimensional axisymmetric computational grid is shown in Figure 3. The convection flow directions were similar in all simulations and an example is given in Figure 4.

Boundary Conditions

For most of the simulations the following boundary conditions were imposed: all boundaries are impervious, with constant temperature along the innermost elements and on the cylinder mantle, and insulated (no heat flow) boundaries on top and bottom of the vessel. Typical isotherm patterns for conduction only, and for convection, are shown in Figures 5a and 5b, respectively. We also examined the case of constant temperature at the top and bottom boundaries, and although the isotherms are different (Figures 5c and 5d), the average heat flow is not very much changed (Table 2, Figure 6). Another variation in boundary conditions was the use of uniform heat flux at the wire heater instead of constant temperature. We found no significant difference compared to constant temperature boundary conditions.

Aspect Ratio

We ran some cases with a different aspect ratio, since the actual geometry of the convecting cells is unknown. These results are shown in Figure 6 and Table 2. For a permeability of 40 darcies, the Nusselt number for a radius to height ratio of 1:6 (that of the experiment) was 2.2, while for a ratio of 2:1, the Nusselt number was 4.8, over twice as large. Thus heat transfer increases considerably with aspect ratio, especially for small aspect ratios (Figure 7).

Size of Temperature Interval

Another variation which we tried was to use a 10°C temperature difference rather than 2°C. The Nusselt number resulting from this case for a permeability of 40 darcies, was only 1.5, considerably less than had been obtained with the smaller temperature difference. This seems logical, since for

a larger temperature interval across the system the region with strongest convective enhancement near the critical point is reduced in volume.

Discretization Effects

Discretization effects result from two sources: from the spacing of the grid points, and from the interpolation of densities and internal energies from tabular data for discrete pressure and temperature values. We found that the first type of discretization effects were not a problem for our simulation. Cases 1 and 2 (Table 2) were identical, except that case 2 had an extra grid point next to the hot wire, to provide improved spatial resolution in the region where discretization effects are strongest. The addition of the extra grid point actually decreased the Nusselt number slightly (Table 2).

Discretization effects resulting from table interpolations were not very great either, but could be significant for a small temperature interval at the critical point. For most of the cases, a table with 1 bar pressure intervals and 0.05°C temperature intervals was used. Another table was constructed with 0.1 bar pressure intervals and 0.1°C temperature intervals, and case 3 (see Table 2) was rerun with this table. For a permeability of 40 darcies, the Nusselt number was 2.2 instead of 2.1. For the case with the 10°C temperature difference, use of the higher resolution table gave nearly identical results.

DISCUSSION

We have developed special numerical techniques to model convective heat transfer at near-critical conditions. Stable steady states were achieved for model systems with linear dimensions of the order of 10 cm, with spatial resolutions better than 1 mm and pressure differences of order 10 Pa between neighboring finite difference grid points.

No validation of the numerical model was possible because the only available experiment on near-critical flow of water in a porous medium (Dunn and Hardee, 1981) lacks sufficiently detailed definition of thermodynamic conditions. Numerical experiments for a flow system similar to that studied by Dunn and Hardee showed significantly enhanced heat transfer near the critical point. However, the enhancements seen in the simulations (up to a factor 5 over pure conduction) are substantially smaller than what was reported from the experiments (up to a factor 70). While we did not expect detailed agreement, a discrepancy that large is surprising and unexplained at the present time. Possible mechanisms for enhanced heat transfer not included in the simulations are thermal dispersion, and flow in channels of high permeability near the wire heater (perhaps generated by dissolution of quartz). In particular, transverse dispersion (Kvernvold and Tyvand, 1980; Hadley, 1982) might have very significant effects for the cylindrical flow geometry considered here, because it produces a component of velocity in the direction of heat transfer (radial).

We suggest that additional carefully controlled and instrumented laboratory experiments should be undertaken to better define the physical conditions and mechanisms for near-critical heat transfer. The cylindrical geometry employed by Dunn and Hardee (1981) is complicated by singular behavior at small radius, and has the undesirable feature that flow behavior may be strongly influenced by conditions (heterogeneities, etc.) on a very small spatial scale. From the standpoint of ease of interpretation a linear flow geometry would be most desirable, but this appears difficult to realize experimentally. The best geometric configuration for experimental studies may be a porous annulus (Prasad et al., 1985; Reda, 1986), where the inner radius is not very much smaller than the outer radius, so that the flow geometry is non-singular and approximately linear. After validation of the numerical model has been achieved, we can look at natural hydrothermal and magma systems and incorporate additional effects such as salinity, fluid-rock interaction, and non-condensible gases.

ACKNOWLEDGEMENT

This work was supported by the Geothermal Technology Division, U.S. Department of Energy, under Contract No. DE-AC03-76SF00098. Robert McKibbin is grateful for the hospitality of the Earth Sciences Division, Lawrence Berkeley Laboratory, while taking part in this work during a period of sabbatical leave from the University of Auckland. The authors are indebted to M. Lippmann for a critical review of the manuscript. Thanks are due to J. Dunn of Sandia National Laboratories for providing us with additional parameters of his laboratory experiments.

REFERENCES

Cappetti, G., Celati, R., Cigni, U., Squarci, P., Stefani, G., and Taffi, L., 1985, Development of Deep Exploration in the Geothermal Areas of Tuscany, Italy, 1985 International Symposium on Geothermal Energy, International Volume, Geothermal Resources Council, 303-309.

Cathles, L. M., 1977, An Analysis of the Cooling of Intrusives by Groundwater Convection which Includes Boiling, *Econ. Geol., 72*, 804-826.

Dunn, J. C. and Hardee, H. C., 1981, Superconvecting Geothermal Zones, *J. Volcanol. and Geotherm. Res., 11*, 189-201.

Facca, G., 1985, Geothermal Activity in Italy, *Geothermal Resources Council Bulletin*, January 1985, 10-14.

Haar, L., Gallagher, J. S., Kell, G. S., 1984, NBS/NRC Steam Tables, Hemisphere Publishing Corp.

Hadley, G. R., 1982, Natural Convection of a Near Critical Fluid through a Porous Medium, Sandia Report SAND82-1072J.

Kvernvold, O., and Tyvand, P., 1980, Dispersion Effects on Thermal Convection in Porous Media, *J. Fluid Mech., 99*, part 4, 673-686.

Norton, D. and Knight, J., 1977, Transport Phenomena in Hydrothermal Systems and Cooling Plutons, *Am. J. Sci., 77*, 937-981.

Prasad, V., Kulacki, F. A. and Keyhani, M., 1985, Natural Convection in Porous Media, *J. Fluid Mech., 150*, 89-119.

Pruess, K., 1983, Development of the General Purpose Simulator MULKOM, Annual Report 1982, Earth Sciences Division, report LBL-15500, Lawrence Berkeley Laboratory.

Reda, D. C., 1986, Natural Convection Experiments with a Finite-Length, Vertical Cylindrical Heat Source in a Water-Saturated Porous Medium, *Nuclear and Chemical Waste Management, 6*, 3-14.

Table 1. Parameters used in Simulations

Parameter	Value
porosity	0.25
permeability	1 to 40 darcies
thermal conductivity	3.35 W/m°C
temperature of wire	377°C
temperature of outer wall	375°C
average pressure	225 bar
cylinder radius	0.0381 m
cylinder height	0.2286 m
aspect ratio (radius : height)	1:6
computational grid (see Fig. 3)	21 x 15
top and bottom boundaries insulating	

Table 2. Results of Critical Convection Simulations

Case	Modifications	Permeability, darcies	Nusselt number Nu
1	coarser mesh*	1	1.039
	average pressure = 230 bars	10	1.211
	temperature interval: 377-379°C	20	1.399
		40	1.694
2	finer mesh (21 x 15)	40	1.493
	average pressure = 230 bars		
	temperature interval: 377-379°C		
3	Average pressure = 225 bars	20	1.854
	temperature interval: 375-377°C	40	2.056
	finer resolution (T,P) table	40	2.227
4	top and bottom boundaries at	20	1.738
	constant temperature	40	2.077
5	aspect ratio 1:3	10	1.795
		20	2.182
		40	2.742
6	aspect ratio 1:2	10	1.945
		20	2.428
		40	3.150
7	aspect ratio 1:1	10	2.198
		20	2.895
		40	3.956
8	aspect ratio 2:1	10	2.313
		20	3.227
		40	4.794
9	temperature interval: 370-380°C	1	1.007
		10	1.150
		20	1.290
		40	1.537
	finer resolution (T,P) table	40	1.531

*the two columns of grid blocks closest to the heater wire were combined

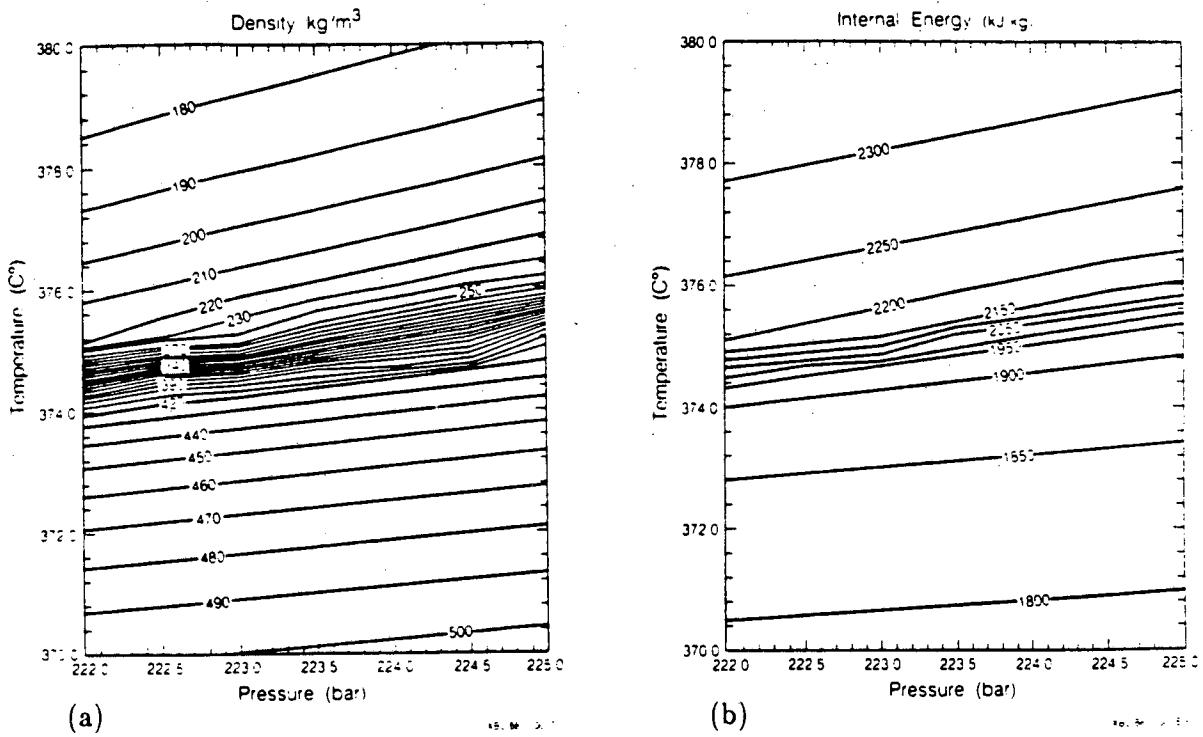

Figure 1. Contours of (a) density (kg/m^3) and (b) internal energy (kJ/kg) for pure water in the critical region.

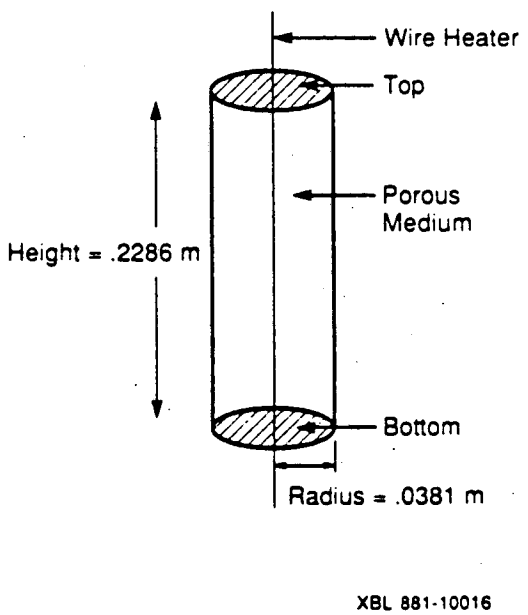

Figure 2. Cylindrical geometry for heat transfer study.

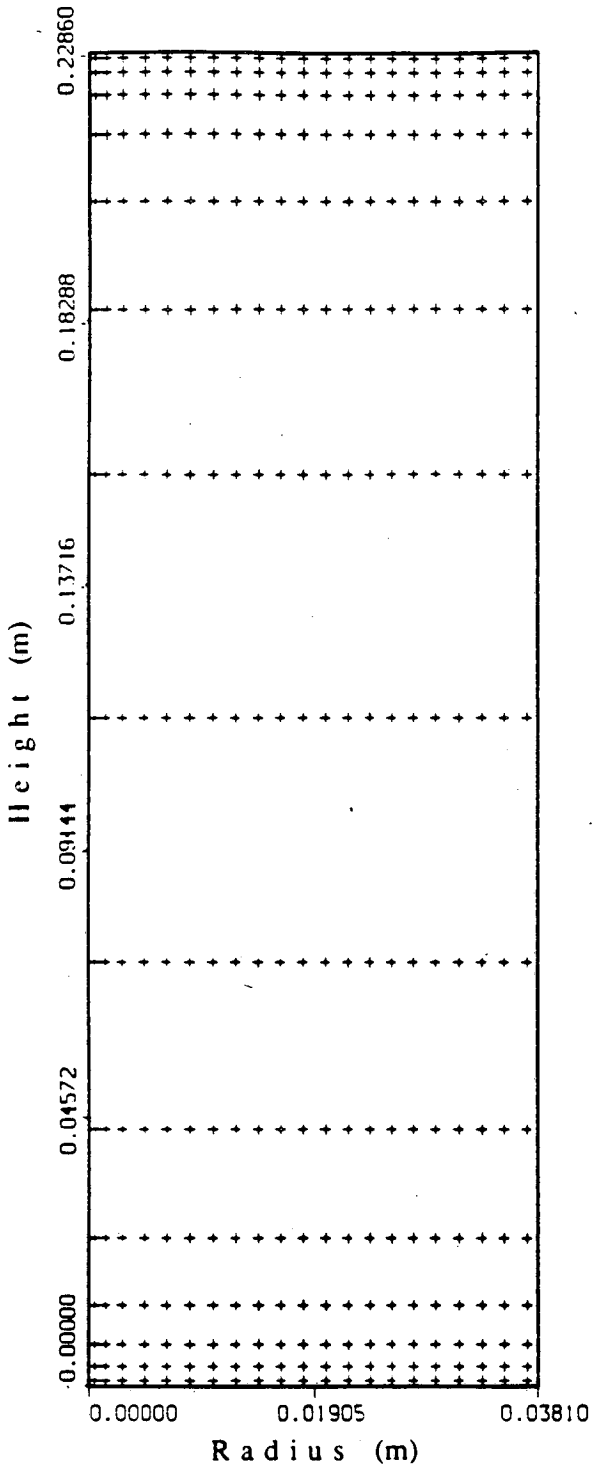

Figure 3. Radial mesh geometry used in simulations. Left hand side of figure is axis of symmetry.

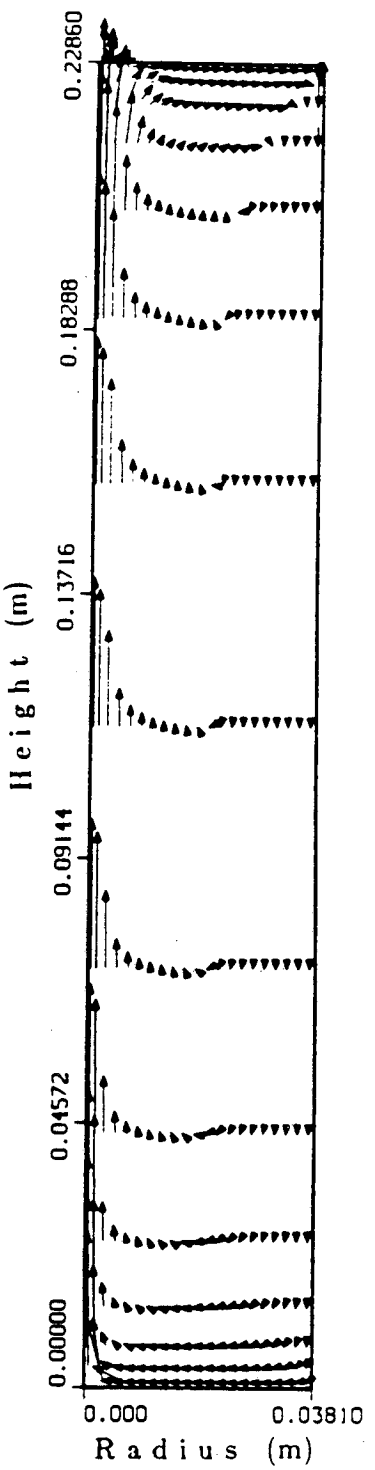

Figure 4. Typical fluid flow vectors (case 3) resulting from simulations of natural convection near the critical point.

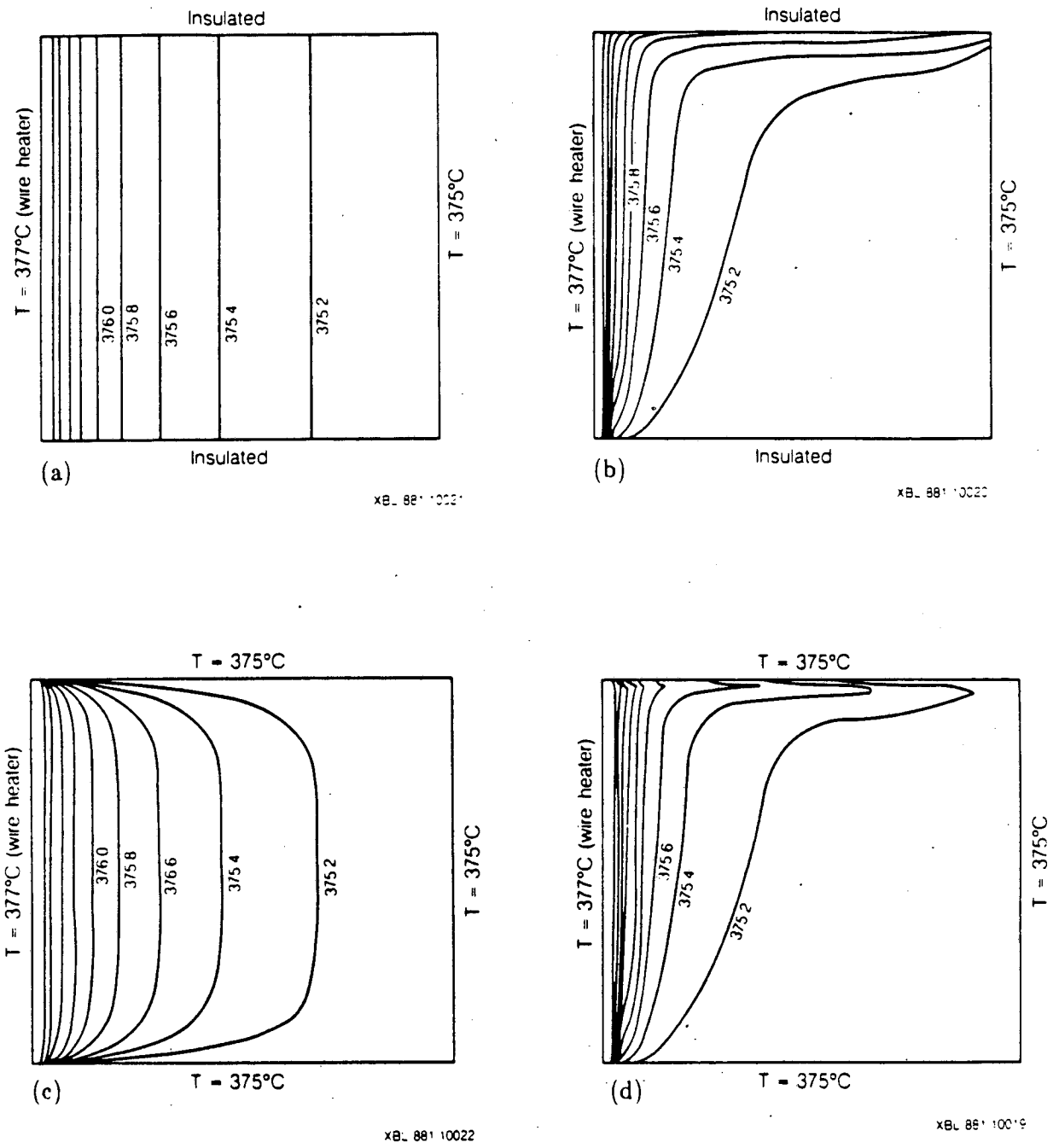

Figure 5. Isotherms for (a) case 2, conduction only (b) case 2, convection, (c) case 4, conduction only and (d) case 4, convection. The radial dimension is exaggerated 6 times.

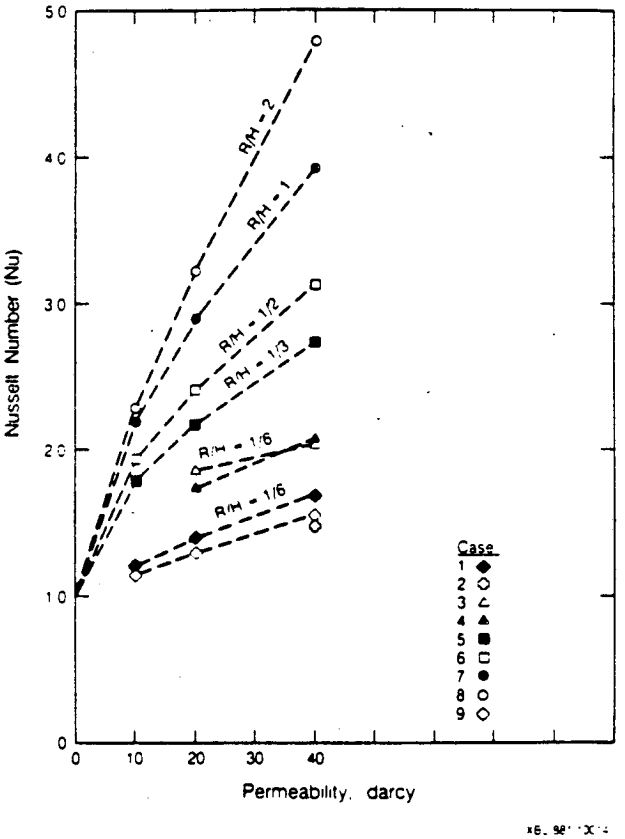

Figure 6. Results of critical convection simulations, plotted in terms of Nusselt number versus permeability (cases described in Table 2).

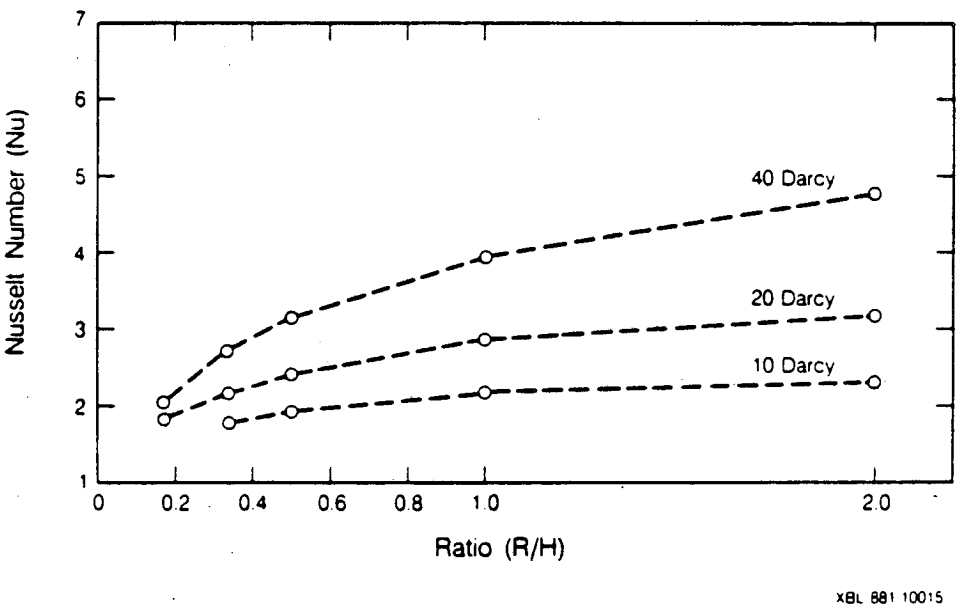

Figure 7. Results of critical convection simulations, plotted in terms of Nusselt number versus aspect ratio (r/H).

LAWRENCE BERKELEY LABORATORY
TECHNICAL INFORMATION DEPARTMENT
UNIVERSITY OF CALIFORNIA
BERKELEY, CALIFORNIA 94720